Received: 20 December 2021 | Revised: 23 September 2022 | Accepted: 7 October 2022

DOI: 10.1002/jcb.30340

RESEARCH ARTICLE

Journal of Cellular Biochemistry WILEY

# Targeting DNA repair to enhance the efficacy of sorafenib in hepatocellular carcinoma

**Mahzeiar Samadaei**[1,2] | **Daniel Senfter**[3] | **Sibylle Madlener**[3] | **Karolina Uranowska**[4,5] | **Christine Hafner**[4,6] | **Michael Trauner**[1] | **Nataliya Rohr-Udilova**[1,2] | **Matthias Pinter**[1,2]

[1]Division of Gastroenterology and Hepatology, Department of Internal Medicine III, Medical University of Vienna, Vienna, Austria

[2]Liver Cancer (HCC) Study Group Vienna, Department of Internal Medicine III, Medical University of Vienna, Vienna, Austria

[3]Department of Pediatrics and Adolescent Medicine, Molecular Neuro-Oncology, Medical University of Vienna, Vienna, Austria

[4]Department of Dermatology, University Hospital St. Poelten, Karl Landsteiner University of Health Sciences, St. Poelten, Austria

[5]Center for Pathophysiology, Infectiology and Immunology, Institute of Pathophysiology and Allergy Research, Medical University of Vienna, Vienna, Austria

[6]Karl Landsteiner Institute of Dermatological Research, Karl Landsteiner Gesellschaft, St. Poelten, Austria

**Correspondence**
Matthias Pinter and Nataliya Rohr-Udilova, Division of Gastroenterology & Hepatology, Department of Internal Medicine III, Vienna Liver Cancer Study Group, AKH & Medical University of Vienna, Vienna, Austria.
Email: Matthias.pinter@meduniwien.ac.at and Nataliya.rohr-udilova@meduniwien.ac.at

**Funding information**
NÖ Forschungs-und Bildungsges.m.b.H (NFB) to Christine Hafner, Grant/Award Number: LSC15-007; Medical Scientific Fund of the Mayer of the city of Vienna to Matthias Pinter, Grant/Award Number: 18123

## Abstract

The multityrosine kinase inhibitor sorafenib remains an important systemic treatment option for hepatocellular carcinoma (HCC). Signaling pathways, which are targeted by sorafenib, are involved in checkpoint and DNA repair response, RAD51 being a candidate protein. Here, we aim to evaluate the effect of the human RAD51 inhibitor B02 in combination with sorafenib in human HCC cells. Impact of *RAD51* expression on HCC patient survival was evaluated by an in silico approach using Human Protein Atlas dataset. Cell viability of HUH7, AKH12, AKH13, and 3P was assessed by neutral red assay. To measure the cytotoxicity, we quantified loss of membrane integrity by lactate dehydrogenase release. We also employed colony formation assay and hanging drop method to assess clonogenic and invasive ability of HCC cell lines upon sorafenib and B02 treatment. Cell cycle distribution and characterization of apoptosis was evaluated by flow cytometry. In silico approach revealed that HCC patients with higher expression of *RAD51* messenger RNA had a significantly shorter overall survival. The RAD51 inhibitor B02 alone and in combination with sorafenib significantly reduced viability, colony formation ability, and invasion capacity of HCC cells. Cell cycle analysis revealed that the combination of both agents reduces the proportion of cells in the G2/M

**Abbreviations:** FBS, fetal bovine serum; FPKM, fragments per kilobase of transcription per million mapped reads; HCC, hepatocellular carcinoma; LDH, lactate dehydrogenase; TBS-T, tris buffered saline with 0.1% Tween20.

Nataliya Rohr-Udilova and Matthias Pinter contributed equally.

phase while leading to an accumulating in the subG1 phase. The RAD51 inhibitor B02 seems to be a promising agent for HCC treatment and enhances the antitumor effects of sorafenib in vitro.

KEYWORDS
B02, DNA repair, hepatocellular carcinoma, RAD51, sorafenib

## 1 | INTRODUCTION

Hepatocellular carcinoma (HCC) is the most common primary malignancy of the liver with a global death rate close to its incidence.[1,2] HCC usually develops in patients with underlying chronic liver disease, predominantly caused by chronic viral hepatitis, alcohol abuse, and nonalcoholic fatty liver disease.[3,4]

The multityrosine kinase inhibitor sorafenib was the first approved drug and the only effective systemic therapy available for HCC for over a decade. Recently, the combination of atezolizumab plus bevacizumab showed improved overall and progression-free survival compared with sorafenib in a phase III trial and represents the new standard of care in systematic front-line therapy.[5–8]

However, given that current second-line agents (i.e., regorafenib, cabozantinib, ramucirumab) have been approved for sorafenib-experienced patients, sorafenib still plays a significant role in the HCC treatment algorithm.[8,9] Sorafenib and other tyrosine kinase inhibitors have known side effects, of which diarrhea and hand-foot skin reactions are probably the most troublesome. Adverse events interfere with the patient's quality of life and often lead to dose reduction or discontinuation.[10] Combination of sorafenib with other agents may allow for dose reduction without decreasing the therapeutic benefit. Combination regimens could also help to overcome chemoresistance and enhance efficacy of sorafenib.[11]

DNA repair genes are upregulated in HCC[12] and are widely considered as a molecular target for cancer therapy.[13,14] The DNA repair machinery is a crucial mechanism to maintain chromosome stability and can be subdivided into two major categories: single-strand break repair and double-strand break repair.[15] Homologous recombination is the major mechanism of double-strand break repair, and RAD51 is the key player in this process. RAD51 binds to DNA and mediates the strand-exchange upon interaction with nucleases, helicases, and DNA translocases.[15] RAD51 inhibition enhances the chemo-/radio-therapeutic effects in a variety of cancers, including HCC.[16–20]

B02 is a highly specific RAD51 inhibitor that binds directly to RAD51 and was identified by high-throughput screening.[21] B02 disrupts homologous recombination as it prevents RAD51 binding to both, single and double stranded DNA.[21] Whereas B02 has been successfully tested in mouse breast cancer and melanoma xenografts,[20,22] there is no data for B02 in HCC.

In the present study, we investigated the anticancer effects of RAD51 inhibitor B02 in different human HCC cell lines and combined it with sorafenib, acknowledging that pathways targeted by sorafenib—including PI3K/Akt and Raf/Mek/Erk,—play a critical role in checkpoint and DNA repair response.[23–25]

## 2 | MATERIALS AND METHODS

### 2.1 | Patient dataset

We used a publicly available human HCC dataset from The Human Protein Atlas[26] to assess the association between *RAD51* expression and patient survival. Patients were classified into two groups according to the Fragments per Kilobase of transcription per million mapped reads value. Median overall survival was determined by Kaplan–Meier method and compared using log-rank tests.

### 2.2 | Cell lines

The human HCC cell line, HUH7 was purchased from Riken Bioresource center (Ibaraki, Japan). The human HCC cell lines AKH12, AKH13, and 3P have been well characterized,[27] and were kindly provided by Prof. Bettina Grasl-Kraupp (institute of Cancer Research, Medical University of Vienna, Austria). HUH7 cells were cultured in Dulbecco's modified Eagle medium (Thermo Fisher Scientific) containing 10% heat inactivated fetal bovine serum (FBS) (Sigma-Aldrich), 1% penicillin-streptomycin (10 000 U/ml) (Thermo Fisher Scientific), and 1% nonessential amino acids (×100) (Thermo Fisher Scientific). AKH12 and AKH13 cell lines were cultured in RPMI-1640 Medium (Sigma-Aldrich) containing 10% heat inactivated FBS. 3P cells were cultured in

RPMI-1640 Medium (Sigma-Aldrich) containing 10% heat inactivated FBS, 5 nM sodium selenit (Sigma-Aldrich), and 30 μM Tocopherol (Sigma-Aldrich).

## 2.3 | Cell viability assay

Cell viability was determined via measuring the uptake of neutral red into lysosomes of viable cells. The cells were seeded into 6-well plates and grown to reach 70%–80% confluency (HUH7 and 3P: $0.8 \times 10^5$ cells per well; AKH12 and AKH13: $1.2 \times 10^5$ cells per well) before treatment with sorafenib (Nexavar, Bayer), B02 (3-(Phenylmethyl)-2-[(1E)-2-(3-pyridinyl)ethenyl]-4(3H)-quinazolinone) (Axon Medchem), or the combination of both. Sorafenib and B02 were dissolved in dimethyl sulfoxide (DMSO). As the sensitivity to sorafenib varied between the cell lines, we aimed to achieve a uniform comparable cell loss of approximately 20% by adjusting sorafenib concentration, according to the dose-response curve for each cell line. Sorafenib concentration chosen in this way (up to 4 μM in test) was then combined with B02. After treatment for 24 h, cells were incubated with 50 μg/ml neutral red in a serum free medium for 2 h at 37°C. Cells were then washed twice with phosphate-buffered saline (PBS) (Thermo Fisher Scientific) and dye taken up by viable cells was dissolved using 1% acetic acid in 70% ethanol. The dye absorbance was measured photometrically at 562 nm. The percentage of viable cells was calculated considering DMSO-treated cells as 100%. DMSO concentration in medium remained below 0.3%.

## 2.4 | Measurements of the lactate dehydrogenase (LDH) activity

LDH release into culture media was measured by a cytotoxicity detection kit from Roche Diagnostics, as described before.[28] LDH-positive control with 100% cell lysis was achieved by addition of Triton X-100. DMSO (Sigma-Aldrich) was used as the vehicle control.

## 2.5 | Colony formation assay

Briefly, cells were seeded in triplicates into 6-well plates at a density of 1000 cells per well and exposed to sorafenib (Nexavar, Bayer), B02 (Axon Medchem), or the combination of both for 24 h in full medium. The drugs were then removed and cells were cultivated in fresh medium. After 7–12 days (cell line dependence) of regular media exchange, colonies were washed with PBS (Thermo Fisher Scientific), fixed with methanol and stained by crystal violet (Merck). Colonies with >50 cells were counted using Bürker-Türk counting chamber. Percentage of survival was calculated considering vehicle-treated samples as 100%.

## 2.6 | Spheroid assay

The hanging drop method was applied to obtain 3D aggregates of cells.[29] Briefly, 24 h treated cells were suspended in a mixture of 70% proper culture medium, 10% FBS (Sigma-Aldrich) and 20% methylcellulose. Drops of 25 μl of the suspension (2000–3000 cells/drop) were distributed equally over a 10 cm petri dish. The plates were incubated upside down overnight at 37°C (5% $CO_2$, 95% humidity) to allow formation of a single stable spheroid. The next day, all hanging drops were collected into a 50 ml falcon tube and embedded into 1.5% rat tail collagen gels (cat. no. 354236; Corning). To prepare the collagen solution according to manufacturer's instruction, we mixed, 3% collagen with an equal volume of 0.85% (wt/vol) methylcellulose in culture medium with 10% FBS (Sigma-Aldrich). The spheroid suspension was pipetted into 24-well plates (350 μl/well), and, incubated for 30 min. Then, the polymerized collagen gels were overlaid with appropriate culture medium containing 0.5% FBS and, incubated at 37°C, 5% $CO_2$ with 95% humidity. ImageJ software and Nikon inverted phase-contrast microscope were used to determine cumulative sprout length per spheroid. For each experiment at least five spheroids were evaluated.

## 2.7 | Cell cycle analysis

The analysis of cell cycle was performed using Propidium Iodide Flow Cytometry Kit (cat. no. ab139418; Abcam) according to manufacturer's protocol. Briefly, HCC cells were seeded in triplicates in 6-well plates and treated with either sorafenib or B02 or with the combination of both. Vehicle (DMSO) treated cells served as control. Cells were harvested by trypsinisation and fixed with 66% Ethanol for 2 h, at 4°C. Cells were then washed with PBS and resuspended in 1X Propidium Iodide + RNase Staining Solution. After incubation for 30 min at 37°C, cells were analyzed for cell cycle distribution with FACS Canto flow cytometer (BD Bioscience) equipped with FlowJo software version 10.6.1 (TreeStar Inc.).

## 2.8 | Apoptosis assay

Annexin V-CF Blue/7-AAD Apoptosis Detection Kit (cat. no. ab214663; Abcam) was used to evaluate the percentage of

live, apoptotic or necrotic cells. The analysis was performed according to manufacturer's instructions. In brief, cells were seeded in triplicates into the 6-well plates and treated by sorafenib, B02, and a combination of both. Vehicle (DMSO) treated cells served as a control. Cells were then harvested, washed with PBS and resuspended in Annexin-binding buffer. Next, cells were incubated in the dark with Annexin V-CF Blue conjugate and 7-AAD Staining Solution for 15 min at room temperature. The samples were analyzed using a FACS Canto flow cytometer (BD Bioscience) equipped with FlowJo software version 10.6.1 (TreeStar Inc.).

### 2.9 | RNA isolation and real-time RT-PCR

Cells were transfected with 50 nM siRNA using Lipofectamine-2000 (Invitrogen) as stated by manufacturer's instructions. After the transfection, messenger RNA (mRNA) was isolated, using Trizol (Thermo Fisher Scientific). To reverse transcribe 1 μg of isolated mRNA, High Capacity cDNA Reverse Transcription Kit (Applied Biosystems) was used. The SYBR-green master mix in StepOnePlus Real-time RT-PCR system (Thermo Fisher Scientific) was used for analysis of gene expression. Relative fold change between *RAD51* (primer sequence forward 5′-GTGGTAGCTCAAGTGGATGG-3′ and reverse 5′-GGGAGAGTCGTAGATTTTGCAG-3′) and *GAPDH* (glyceraldehyde 3-phosphate dehydrogenase) of forward 5′-ACATCGCTCAGACACACCATG-3′ and reverse 5′-TGTAGTTGAGGTCAATGAAGGG-3′) was calculated using the $2^{-ddCq}$ method. Both primers were from Integrated DNA Technologies, IDT.

### 2.10 | Statistical analysis

Microsoft Excel software was used for statistical analysis of the data. The Student's *t* test (unpaired) was used to compare different treatment groups. The values are represented as mean ± standard deviation (*SD*) of three independent experiments. All $p \leq 0.05$ were considered as significant.

## 3 | RESULTS

### 3.1 | *RAD51* expression correlates with HCC prognosis

To evaluate the correlation between *Rad51* expression in HCC tumors and patient survival, we applied an in silico approach. For this, 365 patients from a publicly available HCC dataset[26] were classified into two groups based on the median *RAD51* mRNA expression. HCC patients with high *RAD51* expression showed a significantly shorter median overall survival when compared to the patients with low *RAD51* expression ($p \leq 0.001$) (Figure 1). Thus, increased *RAD51* is associated with poor prognosis in HCC and inhibition of RAD51 may be beneficial.

### 3.2 | Effects of sorafenib in combination with the RAD51 inhibitor B02 on viability and cytotoxicity in human HCC cells

To inhibit RAD51, we applied the small molecule inhibitor B02. Human cultured HCC cells HUH7, AKH12, AKH13, and 3P were treated with increasing concentrations of sorafenib or B02 for 24 h. We measured cell viability using neutral red assay and calculated $IC_{50}$ for B02 and sorafenib (Figure S1). Based on these data, we adjusted incubation time and drug concentrations for the subsequent treatments of each cell line so that viability loss for each single agent remained below 40%. All cell lines were incubated with the adjusted concentrations of sorafenib or B02 or a combination of both for 24 h. Both, sorafenib and B02 reduced cell viability, the effect of combination being additive (Figure 2A–D the middle panel as well as Figure S2A–D the upper panel). Microscopic images of treated cells are shown in the upper panel of Figure 2A–D and support the viability data. The cytotoxicity measured by the LDH release showed similar additive effects for sorafenib and B02 (Figure 2A–D the lower panel as well as Figure S2A–D the lower panel).

To further support the involvement of RAD51 inhibition in the above effects, we silenced *RAD51* expression in all four HCC cell lines by transfection with siRNA. *RAD51* knockdown at mRNA and protein level was confirmed by RT-PCR and western blot analysis (Figure S3B,C).

*RAD51* siRNA silenced cells were then incubated with sorafenib. In line with the previous observations using RAD51 inhibitor B02, siRNA against *RAD51* facilitated the effects of sorafenib in all four HCC cell lines in similar manner (Figure S3A).

### 3.3 | Sorafenib and B02 reduce colony-formation of HCC cell lines

As B02 enhanced the effect of sorafenib on HCC cell viability, we further examined how the same treatment affects the colony formation in HCC cells. As demonstrated in Figure 3, B02 combined with sorafenib significantly reduce the colony formation in three investigated HCC cell lines. Among the cell lines

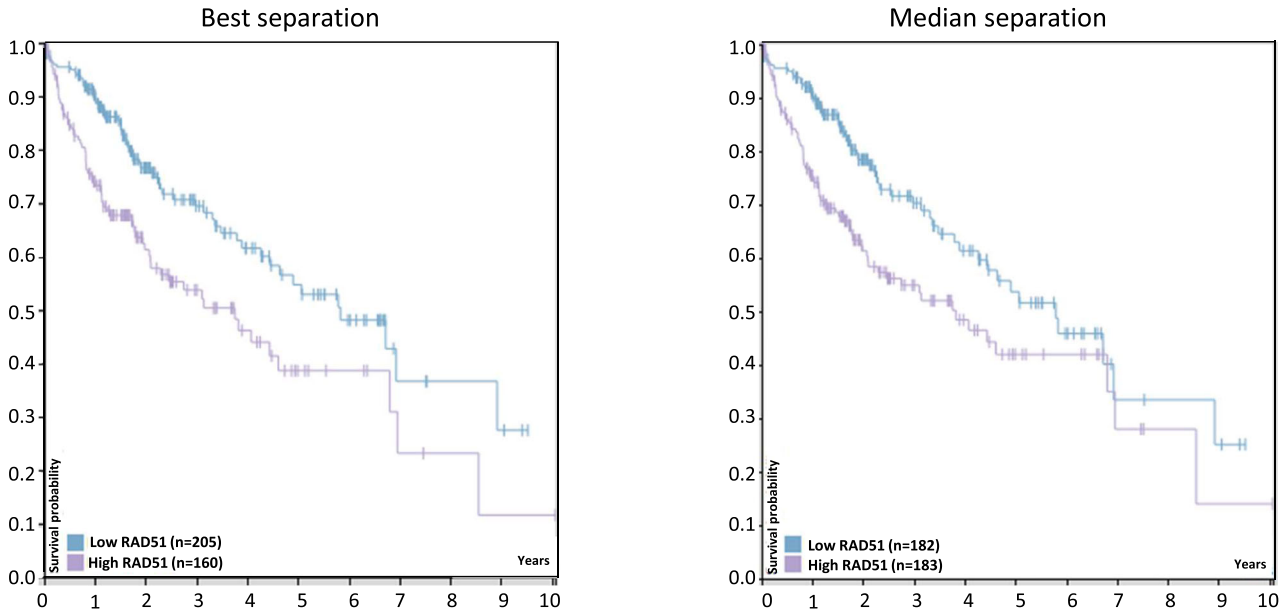


| *RAD51* expression cutoff | 0.9 FPKM | 0.8 FPKM |
|---|---|---|
| 5-year survival high *RAD51* | 39% | 42% |
| 5-year survival low *RAD51* | 53% | 52% |
| Log-rank P value | 9.33e-4 | 2.89e-3 |

**FIGURE 1** Kaplan–Meier overall survival plots for HCC patients stratified according to mRNA expression level of RAD51: best separation (left) and median separation (right). Data from publically available dataset (the Human Protein Atlas) were used ($n = 365$). Log-rank test was applied to compare survival curves. RAD51 expression cutoffs used for group separation, percentage of 5 years survival as well as the corresponding log-rank $p$ value are given. HCC, hepatocellular carcinoma; mRNA, messenger RNA

investigated, colony formation in the AKH12 responded in the most sensitive way to B02 and sorafenib: the combination of 1 μM sorafenib and 10 μM B02 reduced number of colonies by approximately 40% ($p \leq 0.01$) (Figure 3B). Other HCC cell lines 3P and HUH7 required 2 and 3 μM sorafenib, respectively, and higher B02 concentration (15 and 20 μM, respectively) to block colony formation synergistically (Figure 3A and 3C). AKH13 cells did not form colonies in our experimental set up and could not be investigated.

## 3.4 | B02 mitigates intrinsic and sorafenib-induced invasion of HCC cell lines

As conventional 2D cell models do not adequately mimic the three-dimensional tumor growth in vivo, 3D cell culture can be used as a gap-filling assay.[30] Therefore, we assessed the effect of sorafenib and B02 on HCC cell invasion by means of hanging drop method that allows cells to grow three-dimensionally.

Treatment with RAD51 inhibitor B02 completely abolished the HCC spheroid growth in HUH7 from $228 \pm 26\%$ to $123 \pm 27\%$ ($p \leq 0.01$), in AKH12 from $247 \pm 25\%$ to $131 \pm 12\%$ ($p \leq 0.001$), in AKH13 from $252 \pm 14\%$ to $193 \pm 31\%$ ($p \leq 0.05$) and in 3 P from $224 \pm 21\%$ to $121 \pm 11\%$ ($p \leq 0.001$) as compared to vehicle control. Whereas sorafenib even enhanced invasion of all four HCC cell lines as compared to vehicle control, in HUH7 from $228 \pm 26\%$ to $278 \pm 17\%$ ($p \leq 0.05$), in AKH12 from $247 \pm 25\%$ to $295 \pm 25\%$ ($p \leq 0.01$), in AKH13 from $252 \pm 14\%$ to $374 \pm 29\%$ ($p \leq 0.01$) and 3P from $224 \pm 21\%$ to $255 \pm 34\%$ ($p \leq 0.05$) (Figure 4). Interestingly, B02 also abolished sorafenib-induced tumor cell invasion in all cell lines (Figure 4).

## 3.5 | Impact of sorafenib and RAD51 inhibitor B02 on cell cycle and apoptosis in HUH7 tumor cells

To gain insights into the potential mechanism by which sorafenib, B02, and the combination of both reduced

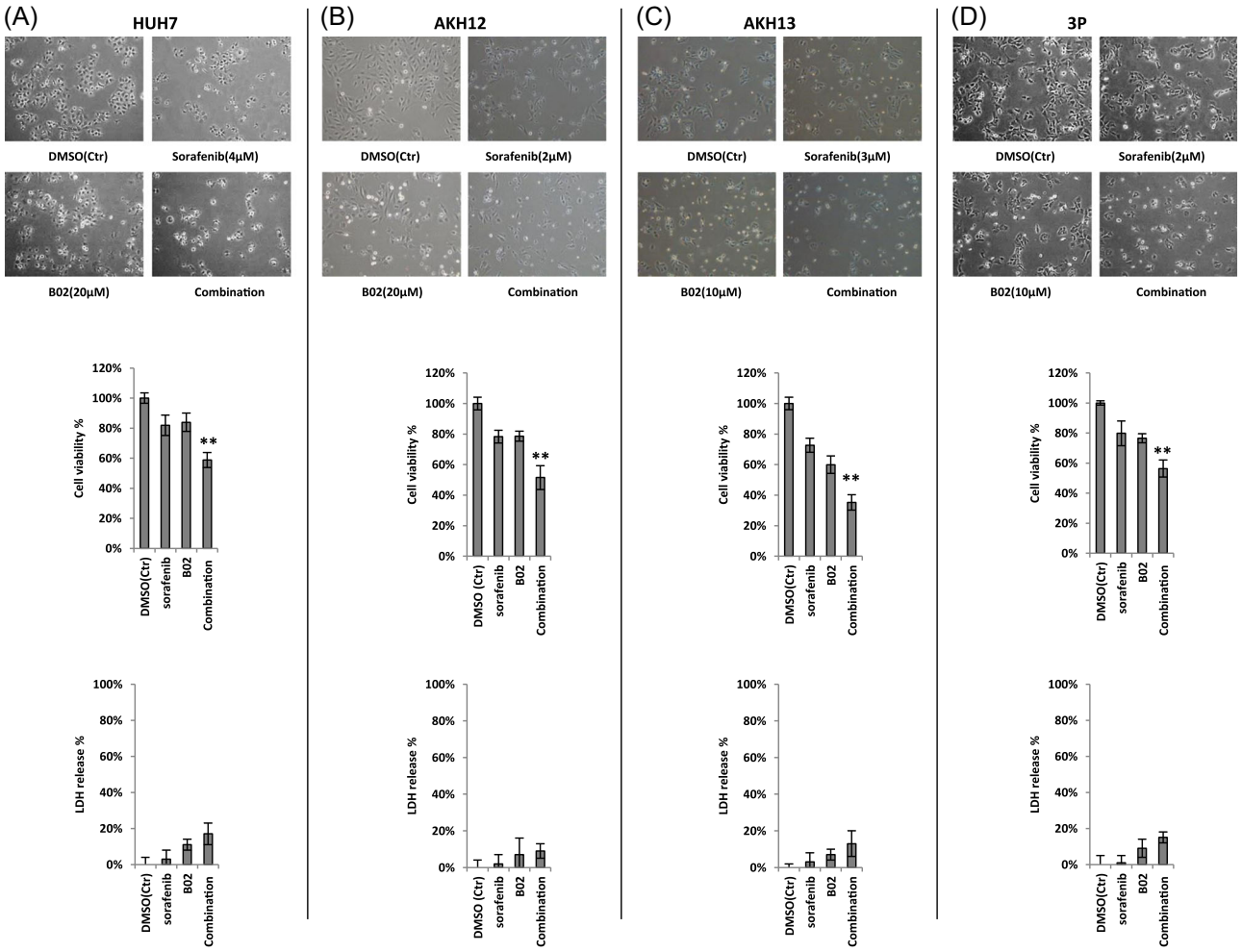


**FIGURE 2** Effects of sorafenib and RAD51 inhibitor B02 on viability and cytotoxicity in HCC cell lines. (A) Upper panel: HUH7 cells were incubated for 24 h with indicated concentration of sorafenib, B02, or combination of both. Cell proliferation inhibition was observed by microscopy. Middle panel: cell viability was analyzed by neutral red assay after 24 h. Lower panel: quantitative measurement of LDH released into the media after 24 h treatment. Cell lysis by Triton X-100 was considered as 100% positive control. (B) The same as A but AKH12 cells were used instead of HUH7. (C) The same as A but AKH13 cells were used. (D) The same as A but 3P cells were used. Data were represented by means ± *SD* from three independent experiences. Standard deviations are indicated by error bars. The *p* values for each combination therapy indicate statistical significance as compared by both individual treatments and analyzed by the Student *t* test (**$p \leq 0.01$). HCC, hepatocellular carcinoma

viability, of HCC cells, we analyzed cell cycle and apoptosis in HUH7 cells.

Cell cycle analysis revealed the following distribution for control cells: subG1 phase (3 ± 1%), G1 phase (44 ± 3%), S phase (35 ± 4%), and G2/M phase (17 ± 3%) (Figure 5A). Upon treatment with sorafenib, cells in G1 phase increased from 44 ± 3% (vehicle control) to 57 ± 3% (sorafenib, $p \leq 0.05$). Upon combination treatment, however, cells accumulated in subG1 phase (3 ± 1% vehicle control vs. 27 ± 3% combination, $p \leq 0.05$), accompanied with a decrease in G2/M phase from17 ± 3% in vehicle control to 2 ± 2% combination treatment ($p \leq 0.05$) (Figure 5A).

We also analyzed apoptosis in HUH7 cells by flow cytometry. HUH7 cells were stained with Annexin V-CF Blue and 7-AAD staining to determine the proportion of viable cells (Annexin V-CF Blue−, 7-AAD−), early apoptotic (Annexin V-CF Blue+, 7-AAD−), late apoptotic/necrotic (Annexin V-CF Blue+, 7-AAD+), as well as dead cells (Annexin V-CF Blue−, 7-AAD+). Interestingly, combination of sorafenib with B02 did not increase the apoptosis rate as compared to each individual treatment (Figure 5B).

To confirm apoptosis-independent cell death, we performed western blotting to evaluate PARP cleavage in HUH7 after sorafenib and/or B02 treatment.

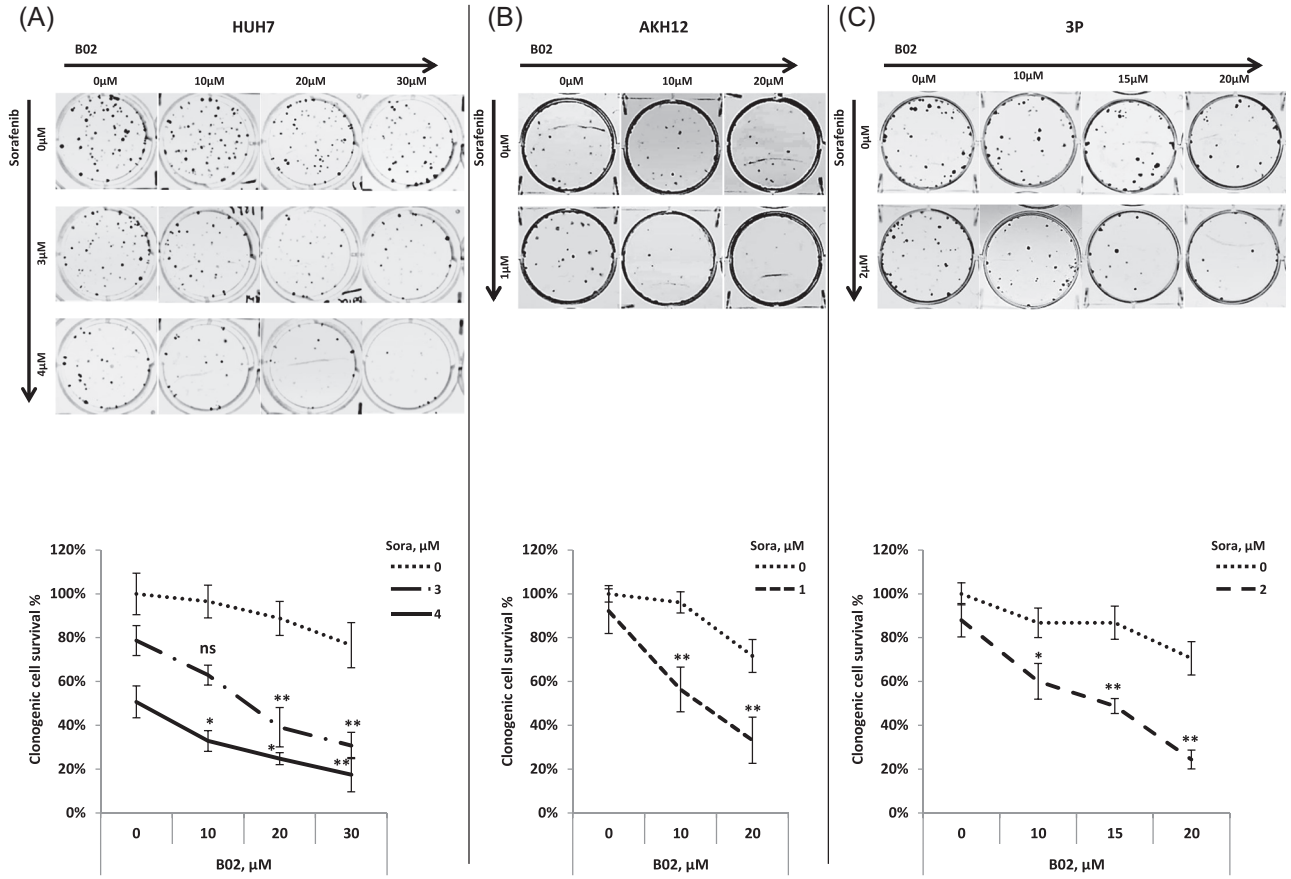


**FIGURE 3** Sorafenib and B02 inhibit colony formation of HCC cells. (A–C) HUH7, AKH12, and 3P were seeded (1000 cells/well) as single cells and then treated with indicated concentration of sorafenib, B02, or in combination for 24 h. The single cells were then monitored for their ability to grow into a colony. The bars represent the clonogenic ability of different groups. Error bars indicate SD obtained from three independent experiments, the percentage of survival was expressed as ratio of survival against that of DMSO-treated cells. Asterisks for each combination therapy indicate statistical significance as compared by both individual treatments and analyzed by the Student *t* test (*$p \leq 0.05$, and **$p \leq 0.01$). DMSO, dimethyl sulfoxide; HCC, hepatocellular carcinoma

In support of FACS data, the results revealed no changes in PARP cleavage (Figure S4A). In line, addition caspase inhibitor Q-VD-OPh that inhibits apoptosis had no impact on cell viability (Figure S4B).

Thus, the combination of sorafenib with B02, increased HUH7 cell death by apoptosis-independent mechanism.

## 4 | DISCUSSION

In the current study, we found that high *RAD51* mRNA expression is associated with shorter survival in HCC patients. Inhibition of RAD51 with a small molecule B02 reduced cell viability, clonogenicity, and invasion in different HCC cell lines. Combination of B02 with sorafenib resulted in additive effects on cell viability and synergetic effects on clonogenicity.

DNA repair contributes to tumorigenicity, chemo- and radioresistance.[15] RAD51 is a central homologous recombination protein for repair of DNA double-strand breaks, which is ubiquitously upregulated in a variety of tumors including HCC, esophageal, pancreatic, breast, lung and colorectal cancer.[31] RAD51 overexpression correlates with tumor growth, metastasis as well as chemo- and radioresistance.[31] RAD51 was also recently linked to immune infiltration in HCC.[32]

DNA repair capacity has a dual role in HCC. Whereas defective DNA repair can result in accumulation of mutations in the host chromosomal DNA thus promoting carcinogenesis,[33,34] its inhibition at later cancer stages may increase susceptibility to treatments by DNA targeting chemotherapeutics and tumor irradiation.[14]

Sorafenib remains an important option in the systemic treatment algorithm of HCC.[8,9] Beside its well-known role in inhibiting tumor cell proliferation and angiogenesis,[35] sorafenib is also linked to DNA damage. For instance, sorafenib activates DNA repair signaling, and inhibition of DNA repair increases sorafenib cytotoxicity in cancers.[36–38]

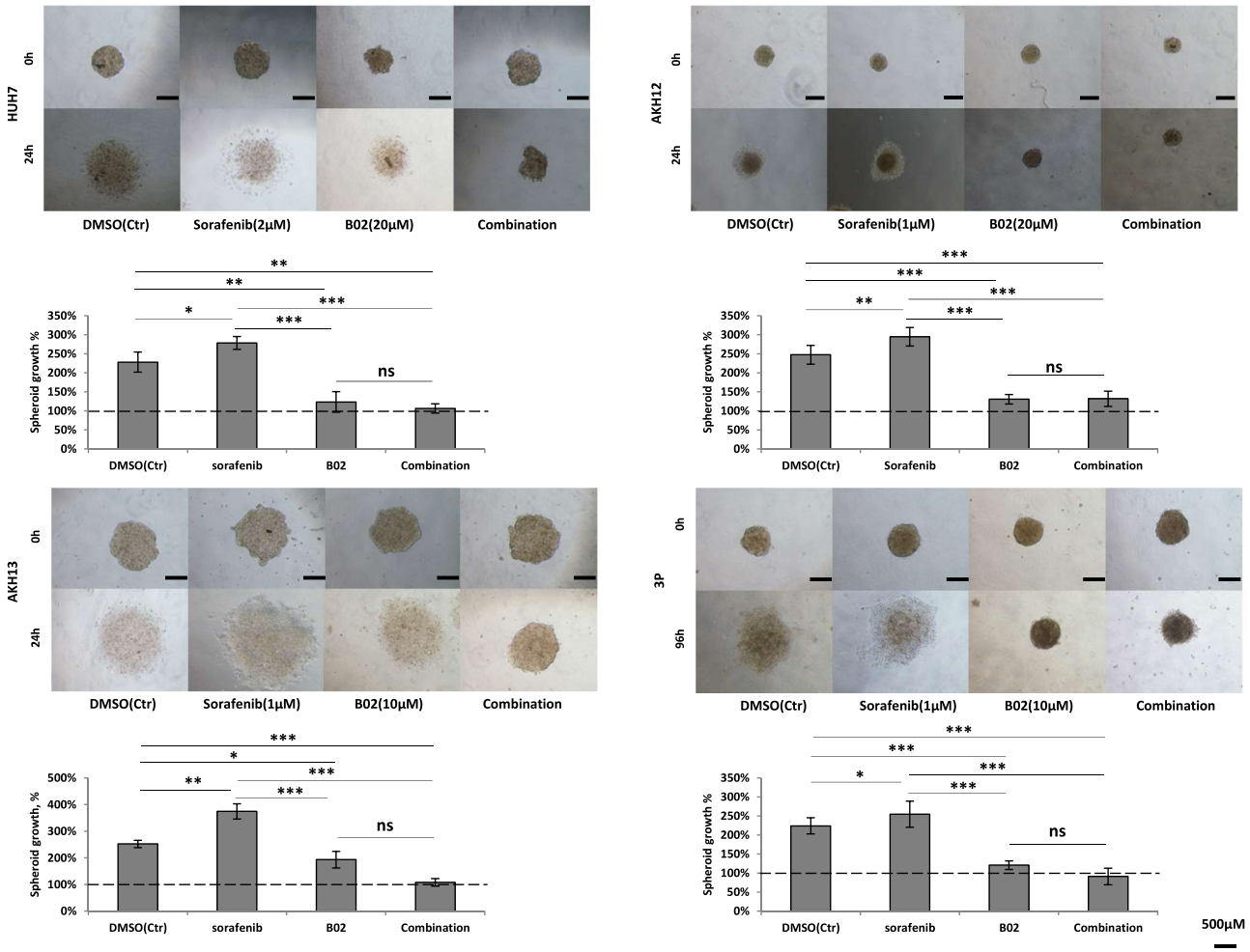


**FIGURE 4** Sprouting assay of HCC cell lines. HUH7, AKH13, and 3P cell lines were treated with sorafenib, B02, or the combination of both for 24 h and then used in the sprouting assay. The areas of spheroids were measured at indicated time points. The quantification of sprouting depth was measured by cumulative sprout length per spheroid using Nikon invaded phase-contrast microscope and ImageJ software, converting pixels to micrometer. The outgrowth rate of combination-treated spheroids was calculated by comparing them to DMSO, sorafenib, and B02 treated ones after indicated time point. At each indicated time point the area of at least 4 spheroids was measured. Error bars indicate mean ± *SD*. The *p* values indicated statistical significance analyzed by the Student *t* test (*$p \leq 0.05$, **$p \leq 0.01$, and ***$p \leq 0.001$). Scale bar, 500 μM. HCC, hepatocellular carcinoma

Inhibition of another DNA repair protein, ataxia telangiectasia mutated, enhanced the effects of sorafenib on hepatoma cells.[36] These findings are in line with our data on cytotoxicity of RAD51 inhibitor plus sorafenib in four different human HCC cell lines (Figure 2A–D, middle panel; Figure S2A–D, upper panel).

We and others have targeted RAD51 in vitro and in vivo by different approaches, such as antisense oligonucleotides, RNA interference, specific DNA aptamers, ribozymes, or small molecule inhibitors (i.e., B02) in different tumor types.[16–20,22] In concordance with our current data in HCC cell lines, targeting RAD51—either directly or indirectly—inhibited proliferation, migration, and invasion of tumor cells.[16–20,22] Antagonism of RAD51 by gefitinib increased antitumor efficacy of irinotecan chemotherapy in HCC cell lines.[17] Notably, *RAD51* knockdown in normal human fibroblast did not enhance sensitivity to cisplatin, which may be indicative of a good safety profile.[39]

B02 is tolerated by mice at doses up to 50 mg/kg without body weight loss.[20,22] This B02 dose was therapeutically active as it potentiated breast cancer cell killing in mouse xenografts.[22] B02 at the same dose also inhibited xenograft melanoma growth in vivo and potentiated the in vitro and in vivo susceptibility of melanoma cells resistant to MAPK inhibitors.[20] Considering B02 molecular weight 339.39 g/mol and 50 mg/kg dose, we estimated maximal B02 concentration being approximately 147 μM. This value exceeds the $IC_{50}$ concentrations for human HCC cells determined in the

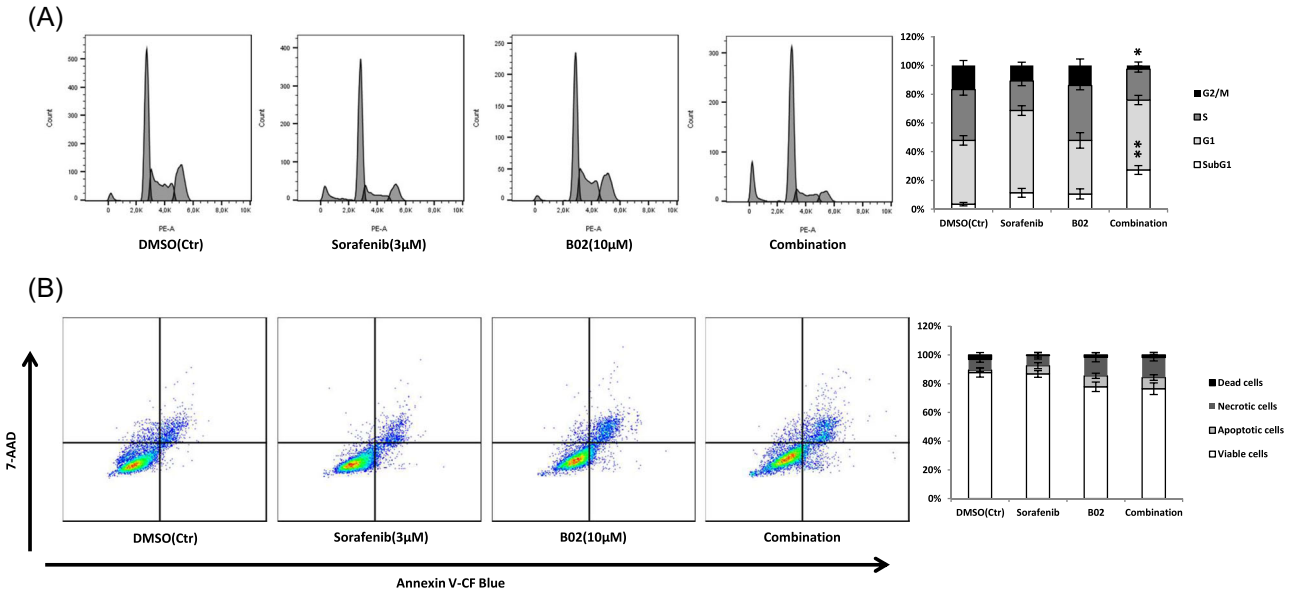


**FIGURE 5** Cell cycle analysis and detection of apoptosis in HUH7 cells exposed to sorafenib and B02 alone or in combination. (A) HUH7 cells exposed to the indicated treatments were assessed for cell cycle distribution by flow cytometry using propidium iodide staining. Representative cytograms (left panel) are reported in bar graphs (right panel). (B) Flow cytometry was used to determine the percentage of intact, apoptotic, necrotic or dead cells upon indicated treatment. Representative cytograms (left panel) are reported in bar graphs (right panel). Error bars indicate mean ± *SD*. The statistical difference represents comparisons of combination-treated cells versus each individual mono-therapy using the Student *t* test (*$p \leq 0.05$ and **$p \leq 0.01$)

current manuscript (Figure S1C) thus supporting the feasibility of B02 applications in HCC xenograft mice models. To our best knowledge, there are no data on application of B02 in humans. However, another RAD51 inhibitor CYT-0851, is currently investigated in a phase I/II trial in advanced solid tumors (clinicaltrials.gov: NCT03997968).[40]

Acknowledging that wild-type P53 physically interacts with RAD51 to suppress homologous recombination,[41] all cell lines used in our study are P53 mutated[42] and exhibited high RAD51 levels.

The absenence of changes in PARP cleavage upon B02 treatment in our study indicates that apoptosis is not the main mechanism of cell death. In line, caspase inhibitor Q-VD-Oph had no impact on cell viability. Necrotic cell death can in part explain cell loss caused by the combination of sorafenib and B02, as accumulation of cells in subG1 and LDH show similar values of approximately 20% in HUH7 cells (Figure 5A and Figure S2A lower panel). However, SubG1 cells could be viable and nonapoptotic and indicate prolonged mitosis, e.g., as observed with low concentrations of paclitaxel, a mitosis targeting drug.[43]

Recent work shows that RAD51 is also involved in mitosis.[44] RAD51 protects under-replicated DNA in mitotic human cells, thus promoting DNA synthesis. We speculate that B02 might inhibit the mitotic RAD51 function thereby slowing down DNA synthesis, prolonging mitosis and leading to the accumulation of cells in the subG1 phase (Figure 5), similar to the observations of others.[43] However, we cannot exclude cell death by other unknown mechanisms which will be elucidated in our next manuscript.

In conclusion, the RAD51 inhibitor B02 enhanced the antitumor effects of sorafenib in four human HCC cell lines. Targeting DNA repair in combination with other approved systemic therapies may become a strategy to overcome chemoresistance in HCC. Further detailed investigations are required to clarify molecular mechanisms behind impaired clonogenicity and invasiveness upon B02 treatment. Our data on B02 and its combination with sorafenib also warrant further evaluation in in vivo HCC models.

## AUTHOR CONTRIBUTIONS

**Mahzeiar Samadaei, Matthias Pinter, and Nataliya Rohr-Udilova**: designed the study concept and interpreted the data. **Mahzeiar Samadaei, Daniel Senfter, Sibylle Madlener, Michael Trauner, Karolina Uranowska, Christine Hafner, Nataliya Rohr-Udilova**: participated in designing the study and analyzing the data. **Mahzeiar Samadaei and Karolina Uranowska**: performed the experiments. **Mahzeiar Samadaei, Nataliya Rohr-Udilova, and Matthias Pinter**: wrote and revised the manuscript. All authors read and revised the manuscript, and approved the final version.

## ACKNOWLEDGMENTS

This study was supported by a grant from the Medical Scientific Fund of the Mayor of the city of Vienna to Matthias Pinter (Project Number: 18123), and by the NÖ Forschungs-und Bildungsges.m.b.H (NFB) to Christine Hafner (Grant Number: LSC15-007).

## CONFLICTS OF INTEREST

MP is an investigator for Bayer, BMS, Lilly and Roche; he received speaker honoraria from Bayer, BMS, Eisai, Lilly, MSD, and Roche; he is a consultant for Astra Zeneca, Bayer, BMS, lpsen, Eisai, Lilly, MSD, and Roche; he received travel support from Bayer, BMS, and Roche. MT received speaker fees from Bristol-Myers Squibb (BMS), Falk Foundation, Gilead, Intercept and Merck Sharp & Dohme (MSD); advisory board fees from Albireo, Boehringer Ingelheim, BiomX, Falk Pharma GmbH, GENFIT, Gilead, Intercept, Janssen, MSD, Novartis, Phenex, Regulus and Shire; travel grants from AbbVie, Falk, Gilead, and Intercept; and research grants from Albireo, CymaBay, Falk, Gilead, Intercept, MSD, and Takeda. He is also coinventor of patents on the medical use of norUDCA filed by the Medical University of Graz. All other authors declare that they have no competing interests.

## DATA AVAILABILITY STATEMENT

The data that support the findings of this study are available from the corresponding authors upon reasonable request. Ethics approval was not required for this in vitro study.

## ORCID

*Mahzeiar Samadaei* http://orcid.org/0000-0003-0842-6578

## REFERENCES

1. McGlynn KA, Petrick JL, El-Serag HB. Epidemiology of hepatocellular carcinoma. *Hepatology*. 2021;73(Suppl 1):4-13.
2. World Health Organization. *CI5: CANCER INCIDENCE IN FIVE CONTINENTS*. [cited 2020 November, 5th]: Available from http://ci5.iarc.fr/Default.aspx
3. Zucman-Rossi J, Villanueva A, Nault JC, Llovet JM. Genetic landscape and biomarkers of hepatocellular carcinoma. *Gastroenterology*. 2015;149(5):1226-1239e4.
4. Akinyemiju T, Abera S, Ahmed M, et al. The burden of primary liver cancer and underlying etiologies from 1990 to 2015 at the global, regional, and national level: results from the global burden of disease study 2015. *JAMA Oncol*. 2017;3(12):1683-1691.
5. Pinter M, Jain RK, Duda DG. The current landscape of immune checkpoint blockade in hepatocellular carcinoma: a review. *JAMA Oncol*. 2021;7(1):113-123.
6. Pinter M, Scheiner B, Peck-Radosavljevic M. Immunotherapy for advanced hepatocellular carcinoma: a focus on special subgroups. *Gut*. 2021;70(1):204-214.
7. Finn RS, Qin S, Ikeda M, et al. Atezolizumab plus Bevacizumab in unresectable hepatocellular carcinoma. *N Engl J Med*. 2020;382(20):1894-1905.
8. Bruix J, Chan SL, Galle PR, Rimassa L, Sangro B. Systemic treatment of hepatocellular carcinoma: an EASL position paper. *J Hepatol*. 2021;75(4):960-974.
9. Pinter M, Peck-Radosavljevic M. Review article: systemic treatment of hepatocellular carcinoma. *Aliment Pharmacol Ther*. 2018;48(6):598-609.
10. Llovet JM, Ricci S, Mazzaferro V, et al. Sorafenib in advanced hepatocellular carcinoma. *N Engl J Med*. 2008;359(4):378-390.
11. Xia S, Pan Y, Liang Y, Xu J, Cai X. The microenvironmental and metabolic aspects of sorafenib resistance in hepatocellular carcinoma. *EBioMedicine*. 2020;51:102610.
12. Yildiz G, Arslan-Ergul A, Bagislar S, et al. Genome-wide transcriptional reorganization associated with senescence-to-immortality switch during human hepatocellular carcinogenesis. *PLoS One*. 2013;8(5):e64016.
13. Gillman R, Lopes Floro K, Wankell M, Hebbard L. The role of DNA damage and repair in liver cancer. *Biochim Biophys Acta, Rev Cancer*. 2021;1875(1):188493.
14. de Almeida LC, Calil FA, Machado-Neto JA, Costa-Lotufo LV. DNA damaging agents and DNA repair: from carcinogenesis to cancer therapy. *Cancer Genet*. 2021;252-253:6-24.
15. Ashour ME, Mosammaparast N. Mechanisms of damage tolerance and repair during DNA replication. *Nucleic Acids Res*. 2021;49(6):3033-3047.
16. Chen CC, Chen CY, Ueng SH, et al. Corylin increases the sensitivity of hepatocellular carcinoma cells to chemotherapy through long noncoding RNA RAD51-AS1-mediated inhibition of DNA repair. *Cell Death Dis*. 2018;9:543.
17. Shao J, Xu Z, Peng X, et al. Gefitinib synergizes with irinotecan to suppress hepatocellular carcinoma via antagonizing Rad51-Mediated DNA-Repair. *PLoS One*. 2016;11(1):0146968.
18. Ward A, Khanna KK, Wiegmans AP. Targeting homologous recombination, new pre-clinical and clinical therapeutic combinations inhibiting RAD51. *Cancer Treat Rev*. 2015;41(1):35-45.
19. Ohnishi T, Taki T, Hiraga S, Arita N, Morita T. In vitro and in vivo potentiation of radiosensitivity of malignant gliomas by antisense inhibition of the RAD51 gene. *Biochem Biophys Res Commun*. 1998;245(2):319-324.
20. Makino E, Fröhlich LM, Sinnberg T, et al. Targeting Rad51 as a strategy for the treatment of melanoma cells resistant to MAPK pathway inhibition. *Cell Death Dis*. 2020;11(7):581.
21. Huang F, Motlekar NA, Burgwin CM, Napper AD, Diamond SL, Mazin AV. Identification of specific inhibitors of human RAD51 recombinase using high-throughput screening. *ACS Chem Biol*. 2011;6(6):628-635.
22. Huang F, Mazin AV. A small molecule inhibitor of human RAD51 potentiates breast cancer cell killing by therapeutic agents in mouse xenografts. *PLoS One*. 2014;9(6):e100993.
23. Wei F, Yan J, Tang D, et al. Inhibition of ERK activation enhances the repair of double-stranded breaks via non-homologous end joining by increasing DNA-PKcs activation. *Biochim Biophys Acta*. 2013;1833(1):90-100.
24. Golding SE, Rosenberg E, Neill S, Dent P, Povirk LF, Valerie K. Extracellular signal-related kinase positively regulates ataxia telangiectasia mutated, homologous

recombination repair, and the DNA damage response. *Cancer Res*. 2007;67(3):1046-1053.
25. Liu Q, Turner KM, Alfred Yung WK, Chen K, Zhang W. Role of AKT signaling in DNA repair and clinical response to cancer therapy. *Neuro Oncol*. 2014;16(10):1313-1323.
26. THE HUMAN PROTEIN ATLAS. *RAD51*. 2021, February 24 [cited 2021 Juni]: Available from https://www.proteinatlas.org/ENSG00000051180-RAD51/pathology
27. Sagmeister S, Eisenbauer M, Pirker C, et al. New cellular tools reveal complex epithelial-mesenchymal interactions in hepatocarcinogenesis. *Br J Cancer*. 2008;99(1):151-159.
28. Samadaei M, Pinter M, Senfter D, et al. Synthesis and cytotoxic activity of chiral sulfonamides based on the 2-azabicycloalkane skeleton. *Molecules*. 2020;25(10):2355. doi:10.3390/molecules25102355
29. Białkowska K, Komorowski P, Bryszewska M, Miłowska K. Spheroids as a type of three-dimensional cell cultures-examples of methods of preparation and the most important application. *Int J Mol Sci*. 2020;21(17):6225. doi:10.3390/ijms21176225
30. Pampaloni F, Reynaud EG, Stelzer EH. The third dimension bridges the gap between cell culture and live tissue. *Nat Rev Mol Cell Biol*. 2007;8(10):839-845.
31. Laurini E, Marson D, Fermeglia A, Aulic S, Fermeglia M, Pricl S. Role of Rad51 and DNA repair in cancer: a molecular perspective. *Pharmacol Ther*. 2020;208:107492.
32. Xu H, Xiong C, Chen Y, Zhang C, Bai D. Identification of Rad51 as a prognostic biomarker correlated with immune infiltration in hepatocellular carcinoma. *Bioengineered*. 2021;12(1):2664-2675.
33. Liang B, Yao S, Zhou J, Li Z, Liu T. Liver resection versus radiofrequency ablation for hepatitis B virus-related small hepatocellular carcinoma. *J Hepatocell Carcinoma*. 2018;5:1-7.
34. Gomez-Moreno A, Garaigorta U. Hepatitis B virus and DNA damage response: interactions and consequences for the infection. *Viruses*. 2017;9(10):304. doi:10.3390/v9100304
35. Wilhelm SM, Adnane L, Newell P, Villanueva A, Llovet JM, Lynch M. Preclinical overview of sorafenib, a multikinase inhibitor that targets both Raf and VEGF and PDGF receptor tyrosine kinase signaling. *Mol Cancer Ther*. 2008;7(10):3129-3140.
36. Fujimaki S, Matsuda Y, Wakai T, et al. Blockade of ataxia telangiectasia mutated sensitizes hepatoma cell lines to sorafenib by interfering with Akt signaling. *Cancer Lett*. 2012;319(1):98-108.
37. Yang XD, Kong FE, Qi L, et al. PARP inhibitor Olaparib overcomes Sorafenib resistance through reshaping the pluripotent transcriptome in hepatocellular carcinoma. *Mol Cancer*. 2021;20(1):20.
38. Wang C, Wang H, Lieftink C, et al. CDK12 inhibition mediates DNA damage and is synergistic with sorafenib treatment in hepatocellular carcinoma. *Gut*. 2020;69(4):727-736.
39. Ito M, Yamamoto S, Nimura K, Hiraoka K, Tamai K, Kaneda Y. Rad51 siRNA delivered by HVJ envelope vector enhances the anti-cancer effect of cisplatin. *J Gene Med*. 2005;7(8):1044-1052.
40. U.S. National Library of Medicine. *ClinicalTrials.gov*: Available from https://clinicaltrials.gov/ct2/show/NCT03997968
41. Linke SP, Sengupta S, Khabie N, et al. p53 interacts with hRAD51 and hRAD54, and directly modulates homologous recombination. *Cancer Res*. 2003;63(10):2596-2605.
42. Caruso S, Calatayud AL, Pilet J, et al. Analysis of liver cancer cell lines identifies agents with likely efficacy against hepatocellular carcinoma and markers of response. *Gastroenterology*. 2019;157(3):760-776.
43. Demidenko ZN, Kalurupalle S, Hanko C, Lim CU, Broude E, Blagosklonny MV. Mechanism of G1-like arrest by low concentrations of paclitaxel: next cell cycle p53-dependent arrest with sub G1 DNA content mediated by prolonged mitosis. *Oncogene*. 2008;27(32):4402-4410.
44. Wassing IE, Graham E, Saayman X, et al. The RAD51 recombinase protects mitotic chromatin in human cells. *Nature Communications*. 2021;12(1):5380.

## SUPPORTING INFORMATION

Additional supporting information can be found online in the Supporting Information section at the end of this article.

**How to cite this article:** Samadaei M, Senfter D, Madlener S, et al. Targeting DNA repair to enhance the efficacy of sorafenib in hepatocellular carcinoma. *J Cell Biochem*. 2022;123:1663-1673. doi:10.1002/jcb.30340